RSC Applied Polymers

ROYAL SOCIETY OF CHEMISTRY

COMMUNICATION

View Article Online
View Journal | View Issue

Cite this: *RSC Appl. Polym.*, 2024, **2**, 816

Received 23rd August 2023,
Accepted 1st June 2024

DOI: 10.1039/d3lp00141e

rsc.li/rscapplpolym

Preparation of gradient porous polymer membranes with multifunctionality†

Weigang Ji, Xiaohu Li, Qi Xi, Mengyuan Song, Xue Wu and Pengfei Song *

Porous membranes have attracted considerable attention in materials science. It is crucial to develop a simple strategy for multifunctional porous membranes with broad applications. Herein, gradient porous membranes were prepared from a poly(ionic liquid) (PIL) of poly[3-cyanomethyl-1-vinylimidazolium bis(trifluoromethane-sulfonyl)imide] and the natural small molecule of α-thioctic acid (TA) using a combination of solution mixing, ring-opening polymerization (ROP) and post-processing. The resulting membranes of PIL/PTA with gradient pores were confirmed by FT-IR, NMR, Raman, and SEM characterizations. Interestingly, PIL/PTA porous membranes are stimulus-responsive materials with self-healing and UV-blocking properties. It is demonstrated that polymer membranes with solvent-stimulated responsiveness depend mainly on their gradient pore structure, which can be used as a highly sensitive solvent sensor. In addition, self-healing and UV-blocking properties have been developed by combining typical features of PIL and PTA into porous membranes. This work is beneficial for the rational design of multifunctional porous membrane materials to meet existing applications.

Porous polymer membranes have been utilized in various applications such as adsorption, separation, catalysis, and energy storage.[1–3] It is reported that these promising materials can be prepared using template-free and template-based strategies.[4,5] However, the template-free strategy using condensation or other C–C coupling reactions is usually considered a time-consuming and labor-intensive process.[6] The template-based method for porous polymer membranes was often limited to membrane porosity with a single structural level and the pore collapse due to the removal of the template.[7] It is difficult to produce polymer membranes with different porous structures using traditional methods.[8] Moreover, there is an increasing demand for the fabrication of porous polymer membranes with multifunctional properties to meet specific purposes.[9–11] Therefore, it is essential to develop facile approaches to obtain novel porous polymer membranes with multifunctionality.

Recently, the preparation of porous polymer membranes from poly(ionic liquids) (PILs) has attracted worldwide interest as the unique properties of PILs are incorporated into these macromolecular architectures, facilitating the expansion of the property/function window of PILs and traditional porous polymer membranes. For example, Yuan's group prepared highly charged porous polymer membranes with a tunable pore size and gradient pore structure, which depends on the electrostatic complexation between imidazole-based cationic PILs and multivalent benzoic acid derivatives.[12] Yuan's group also reported that gradient porous structured membranes were obtained from PILs and polyacrylic acid (PAA) and exhibited excellent stimulus response to organic solvents.[13] Furthermore, Wang *et al.* proposed a one-step method for the synthesis of supramolecular porous polyelectrolyte membranes (SPPMs) from a single PIL, based on the hydrogen-bond-induced phase separation of the PIL between its polar and apolar domains.[14] It is demonstrated that PILs can be effectively used for the fabrication of porous polymer membranes.[1–24]

In addition, significant effort has been devoted to the rational design of porous polymer membranes with different functions, contributing to their versatility and application potential.[15–17] Among these, self-healing is one of the attractive properties for membrane materials, allowing mechanical damage to be repaired without external assistance. However, the construction of functional porous polymer materials with self-healing ability still remains a challenge, which often requires the introduction of multiple levels of non-covalent bonds into polymer frameworks to exhibit reversible association–dissociation behavior. Recently, a natural small

College of Chemistry and Chemical Engineering, Key Laboratory of Eco-functional Polymer Materials of the Ministry of Education, Key Laboratory of Eco-environmental Polymer Materials of Gansu Province, Gansu International Scientific and Technological Cooperation Base of Water-Retention Chemical Functional Materials, Northwest Normal University, Lanzhou 730070, China. E-mail: songpf@nwnu.edu.cn

†Electronic supplementary information (ESI) available: Experimental section and supplementary figures. See DOI: https://doi.org/10.1039/d3lp00141e

molecule of α-thioctic acid (TA) has been investigated for the design of multifunctional materials with self-healing capability, which depends on the unique structure of TA with disulfide bonds and carboxyl groups.[18–20] For example, Wu's group reported that an ionic gel paint was prepared by the concentration-induced autonomous ring-opening polymerization of TA under ambient conditions. It is found that the addition of ionic liquids prevents further depolymerization of poly (α-thioctic acid) (PTA) by forming hydrogen bonds, resulting in a super stretched ionic gel with highly tunable mechanical and conductive self-healing properties.[21] Wang's group reported the preparation of a dynamic ionic liquid with TA for intelligent sensing devices, which can be easily repaired within 20 minutes and return to the original mechanical properties.[22] Accordingly, it is significant to the reasonable development of PIL and TA for multifunctional porous polymer membrane materials with self-healing properties.

Herein, we described that a strategy was developed for porous polymer membranes from PIL and TA with the combination of solution mixing, ring-opening polymerization, and post-processing. The prepared polymer membranes with gradient porous structure were determined by FT-IR, NMR, Raman, and SEM characterizations. Moreover, gradient porous membranes exhibited multifunctionality including solvent-stimulated responsiveness, self-healing, and UV-blocking properties. It is demonstrated that the solvent-stimulated responsiveness of polymer membranes was due to the gradient porous structure. Meanwhile, the self-healing and UV-blocking properties depend largely on the cooperative effect of PIL and PTA in the polymer network. The work described here paves the way for the rational design of multifunctional porous membranes.

We aim to fabricate multifunctional porous polymer membranes by phase separation of electrostatically cross-linked polymer networks from PIL (Fig. 1a). Thus, the strategy from hydrophobic PIL and hydrophilic TA with the combination of solution mixing, ring-opening polymerization, and post-processing was developed as shown in Fig. 1b (details were provided in ESI†). First, the PIL of poly[3-cyanomethyl-1-vinylimidazolium bis(trifluoromethane sulfonyl)imide] was well synthesized (Fig. S1, ESI†). PIL and TA solutions were then prepared and mixed at room temperature. PIL/PTA complex membrane can be developed by further drying the mixed solution. This is because the heat-induced ring-opening polymerization of TA readily occurs during this process (Fig. S2 and S3, ESI†). Moreover, the porous architecture of the PIL/PTA membrane was easily developed by the soaking treatment of the polymer composites with ammonia, owing to the formation of an electrostatic cross-linking network between hydrophobic PIL and neutralized PTA, as well as the presence of phase separation of the PIL/PTA complex in ammonia solution (Fig. S4, ESI†). Accordingly, PIL/PTA membranes can be developed from PIL and TA at different weight percentages (Table S1, ESI†). It is noted that the surface of the prepared porous membrane in direct contact with the mold substrate is referred to as the "bottom" surface, while the other side is referred to as the "top" surface (Fig. 1c).

To investigate the structure of PIL/PTA membranes, scanning electron microscope (SEM) was used for the microstructural observation as shown in Fig. 2. It is clear that the pore structure was present in the cross-section of PIL/

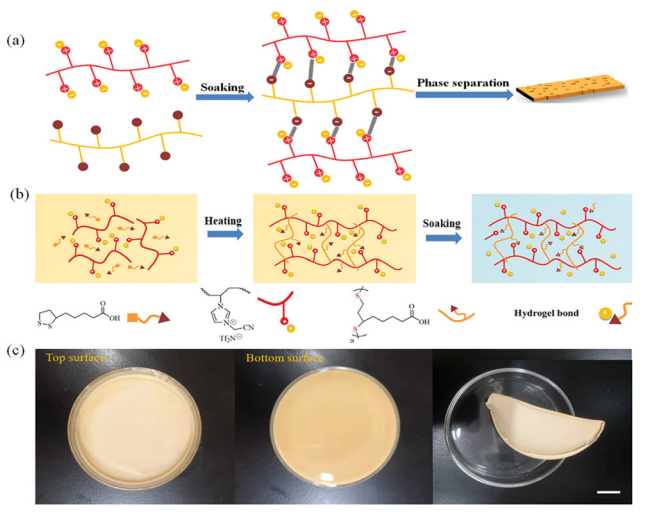

Fig. 1 (a) Strategy for the fabrication of porous polymer membrane. (b) Schematic of the preparation of the porous PIL/PTA membrane. (c) Digital photographs of porous membrane of PIL/PTA-5; scale bar: 2 cm.

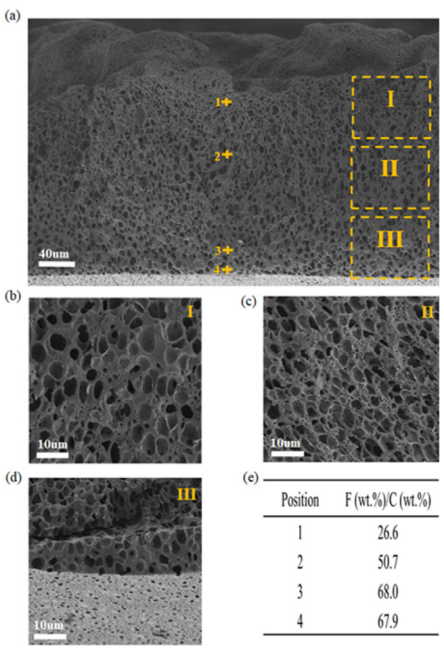

Fig. 2 (a) SEM image of the cross-section of the PIL/PTA-5 membrane. (b)–(d) Cross-sections of PIL/PTA-5 membranes derived from the top layer (I), middle layer (II) and bottom layer (III). The pore sizes gradually decrease from the top layer (zone I, average pore size 7.51 ± 0.53 μm) to middle layer (zone II, average pore size 4.52 ± 0.62 μm) to bottom layer (zone III, average pore size 1.06 ± 0.70 μm). (e) Fluorine element content at different locations (marked in a) in the cross-section of PIL/PTA-5 membrane.

PTA-5 membrane (Fig. 2a), with the pore size decreasing from the top to the bottom, indicating that the gradient porous membrane was well developed (Fig. 2b–d). The construction of gradient porous architectures mainly depends on the ammonia treatment process of the PIL/PTA complex membrane.[12,13] An electrostatic cross-linking network can be formed with the hydrophobic PIL and the neutralized PTA in an ammonia solution. At the same time, the diffusion of water solution into the PIL/PTA membrane induced the phase separation of hydrophobic PIL and neutralized PTA, facilitating the formation of pores in the polymer complex membrane. It is found that the water diffusion leads to the release of hydrophobic fluorinated anions (Tf_2N^-) from the top surface to the bottom surface of the PIL/PTA membrane in the mold. As shown in Fig. 2e, the mass ratio of fluorine to the carbon contained along the cross-section of the PIL/PTA-5 membrane increased from 26.6 wt% at the top to 67.9 wt% at the bottom, which was directly related to the gradient pore distribution. It is suggested that the thicker membrane of PIL/PTA-5 with more hydrophobic fluorinated anions favors the formation of gradient porous structures. Comparatively, the polymer complex membrane prepared from poly[1-cyanomethyl-3-vinylimidazolium bromide] and TA exhibits uneven pores distribution (Fig. S5, ESI†), which owing to the PIL with hydrophilic anions is unsuitable for the phase separation process in water. It is demonstrated that gradient porous membranes can be well developed from hydrophobic PIL and TA with the combination of solution blending, ring-opening polymerization, and ammonia treatment.

The thermal behavior and mechanical performance of PIL/PTA membranes were investigated in detail. Thermogravimetric analysis results showed that porous PIL/PTA membranes exhibited good thermal stability, with the decomposition temperatures of $T_{d,-5\%}$ (5% weight loss temperature) $T_{d,max}$ (maximum weight loss temperature) above 200 °C and 300 °C respectively (Fig. S6, ESI†). The mechanical properties test indicated that porous membranes of PIL/PTA exhibit high tensile strength (Fig. S7, ESI†). It is shown that the tensile strength of porous membranes increased with the increasing content of PIL, with the highest tensile strength of PIL/PTA-5 reaching 92.86 kPa. In addition, PIL/PTA membranes are highly flexible and can be folded easily for practical applications.

The solvent stimulus-responsive performance of PIL/PTA membranes was investigated in detail. As shown in Fig. 3a, the porous membrane of PIL/PTA-5 was highly responsive to acetone vapor, quickly bending from its flat state into a loop with the top surface bending inward, resulting in a bending angle of θ = 360° in 9 s (ESI Movie 1†). The fast actuation of polymer membrane mainly depends on the gradient porous structure favor for the solvent interaction with acetone solution. It is considered that the bottom surface region of the gradient polymer membrane with more fluorinated anions (Tf_2N^-) is more solvated by acetone compared with the top surface, which allows the bending of PIL/PTA membranes in the presence of acetone vapor. In addition, the PIL/PTA-5 membrane also responded to acetonitrile vapor with the shape bending. However, the bending direction of the porous membrane with acetonitrile is opposite to that in acetone solvent (Fig. S8, ESI†). This is due to the PTA component of the gradient porous membrane being more readily solvated by acetonitrile compared to PIL (Fig. S9, ESI†). It is suggested that the PIL/PTA-5 membrane with high solvent-response capacity can be used for the visual discrimination between acetone and acetonitrile solvents.

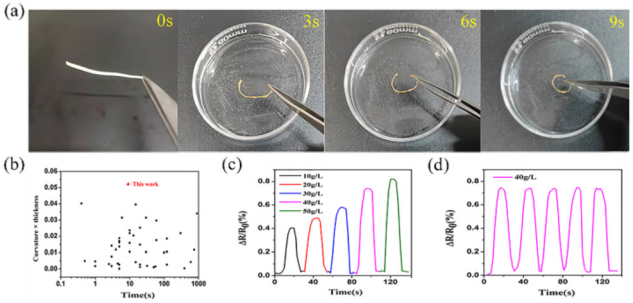

Fig. 3 (a) Stimulus-responsive process of the PIL/PTA-5 membrane in acetone vapor. (b) The actuation speed of PIL/PTA-5 compared with previous reports. (c) Solvent sensing tests based on PIL/PTA-5 membranes for the different concentrations of acetone solutions from 10 g L^{-1} to 50 g L^{-1}. (d) The stability of PIL/PTA-5 as a solvent sensor.

Furthermore, the acetone actuation performance of PIL/PTA membranes with different compositions was also investigated. Porous membranes with high PIL content have a fast actuation speed, which is due to the strong solvent effect between PIL and acetone (Fig. S10, ESI†). The curvature corresponding to the thickness of bending membranes was summarized to demonstrate the response performance of the PIL/PTA membrane (Table S2, ESI†). Since the bending curvature scales inversely with the membrane thickness, we plot "curvature × membrane thickness" *versus* time (Fig. 3b). It is obvious that the PIL/PTA-5 membrane, with the high content of PIL, has a high curvature and actuation rate (Table S3, ESI†). Thus, the PIL/PTA-5 membrane actuator can well simulate the rapid stimulus response performance of mimosa (Fig. S11 and ESI Movie 2†). In addition, the PIL/PTA-5 membrane can be used as a highly sensitive solvent sensor (Fig. 3c and d), showing a response concentration of 10 g L^{-1} towards 50 g L^{-1} acetone with a response time of 8 s (Fig. S12, ESI†).

Porous membranes with the self-healing capability are extremely attractive to the emerging application of smart materials. Thus, self-healing performance of PIL/PTA-5 membrane was investigated in detail. As shown in Fig. 4a, the self-healing process of broken membranes can be well developed with acetone solution (Fig. 4b and ESI Movie 3†). It is shown that the self-healing membrane has almost the same stimulus-response ability as the original PIL/PTA-5 (Fig. 4c). In addition, glass transition temperature (T_g) and mechanical properties of the self-healing membrane were investigated as shown in Fig. S13 and S14, ESI.† The results

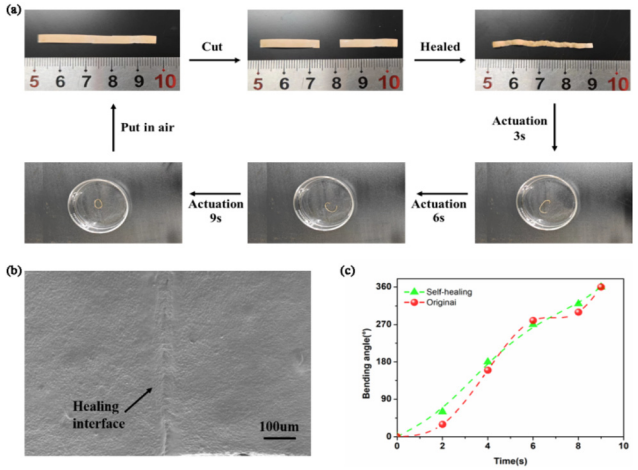

Fig. 4 (a) Photographs of the self-healing process of the PIL/PTA-5 membrane and the re-stimulation response process of the PIL/PTA-5 membrane after self-healing. (b) SEM image of the healing interface of the PIL/PTA-5 membrane. (c) Dependence of the bending angle against time when the original PIL/PTA-5 membrane and self-healing sample are placed in acetone vapor.

showed that the PIL/PTA-5 membrane has a designed self-healing capability. It is considered that the self-healing capability of PIL/PTA porous membrane mainly depends on the induction effect of acetone, leading to the reconstruction of dynamic disulfide bond and electrostatic interaction between PIL and neutralized PTA in the polymer network. Moreover, the porous structure of the PIL/PTA-5 membrane remains undamaged after 10 times bending/debending tests with the acetone stimulation (Fig. S15, ESI†). It is demonstrated that PIL/PTA membranes exhibit high stability in organic solvents (Fig. S16, ESI†).

The development of UV-shielding membrane materials from PIL and PTA is of great importance, as PTA with dynamic disulfide bonds should have high ultraviolet resistance.[23] Thus, the UV transmittance values of PIL, PTA, and PIL/PTA membranes were determined as shown in Fig. 5a, which indicates that the porous membrane has excellent ultraviolet shielding ability with transmittance values less than 7%. It is found that PTA with dynamic disulfide bonds exhibits high ultraviolet resistance, while PIL with imidazole groups has low ultraviolet resistance.[24] Therefore, the UV-blocking capacity of

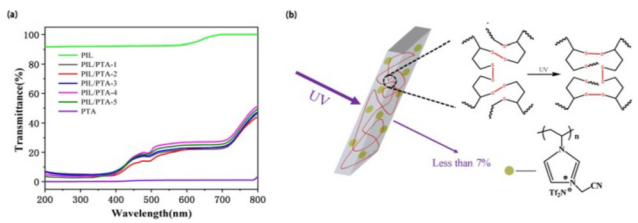

Fig. 5 (a) UV-vis transmittance spectrum of the PIL/PTA membrane (membrane thickness = 0.25 mm). (b) The UV resistance mechanism of the PIL/PTA membrane.

porous membranes is due to the combination of typical properties of PIL and PTA, which mainly depends on PTA, resists ultraviolet radiation through the reversible breaking and rebuilding process of dynamic disulfide bonds (Fig. 5b).†

In conclusion, gradient porous membranes with stimulus-responsive, self-healing, and UV-blocking ability were successfully fabricated by a simple concept of incorporating PTA into a poly(ionic liquid) network. The strategy combining solution mixing, ring-opening polymerization, and post-processing was developed for gradient porous membranes. The resulting porous membranes exhibit high stimulus-responsiveness and self-healing capability. In addition, PIL/PTA membranes have excellent UV-blocking ability with UV transmittance values less than 7%. It is demonstrated that multifunctional porous membranes have been well developed from PIL and TA with the potential for smart sensing, self-healing, and UV-shielding materials.

Conflicts of interest

There are no conflicts to declare.

Acknowledgements

The authors gratefully acknowledge the financial support from NSFC (22161040, 21564013), NWNU (NWNU-LKZD2021-3).

References

1 C. C. Duan, R. Kee, H. Y. Zhu, N. Sullivan, L. Z. Zhu, L. Z. Bian, D. Jennings and R. O'Hayre, *Nat. Energy*, 2019, **4**(3), 230–240.
2 J. S. Zhang, J. A. Schott, S. M. Mahurin and S. Dai, *Small Methods*, 2017, **1**(5), 1600051.
3 J. Liang, Z. Q. Song, S. Y. Wang, X. L. Zhao, Y. H. Tong, H. Ren, S. L. Guo, Q. X. Tang and Y. C. Liu, *ACS Appl. Mater. Interfaces*, 2020, **12**(47), 52992–53002.
4 Y. Q. Yang, C. Y. Chuah, L. N. Nie and T. H. Bae, *J. Membr. Sci.*, 2019, **569**, 149–156.
5 M. Radjabian and V. Abetz, *Prog. Polym. Sci.*, 2020, **102**, 101219.
6 K. V. Peinemann, V. Abetz and P. F. W. Simon, *Nat. Mater.*, 2007, **6**(12), 992–996.
7 S. Petcher, D. J. Parker and T. Hasell, *Environ. Sci.: Water Res. Technol.*, 2019, **5**, 2142–2149.
8 A. K. Kheirabad, X. J. Zhou, D. J. Xie, H. Wang and J. Y. Yuan, *Macromol. Rapid Commun.*, 2021, **42**(8), 2000143.
9 Z. Sheng, J. Zhang, J. Liu, Y. Zhang, X. Chen and X. Hou, *Chem. Soc. Rev.*, 2020, **49**, 7907–7928.
10 Y. Li, Y. Linghu and C. Wu, *ACS Appl. Mater. Interfaces*, 2020, **12**(17), 20096–20102.
11 B. Wang, Q. Wang, Y. Wang, J. Di, S. Miao and J. Yu, *ACS Appl. Mater. Interfaces*, 2019, **11**(46), 43409–43415.

12 Q. Zhao, J. W. C. Dunlop, X. L. Qiu, F. H. Huang, Z. B. Zhang, J. Heyda, J. Dzubiella, M. Antonietti and J. Y. Yuan, *Nat. Commun.*, 2014, **5**, 1–8.
13 H. Lin, J. Gong, H. Miao, R. Guterman, H. Song, Q. Zhao, J. W. C. Dunlop and J. Yuan, *ACS Appl. Mater. Interfaces*, 2017, **9**(17), 15148–15155.
14 Y. Shao, Y. L. Wang, X. S. Li, A. K. Kheirabad, Q. Zhao, J. Y. Yuan and H. Wang, *Angew. Chem., Int. Ed.*, 2020, **59**(39), 17187–17191.
15 Y. Liang, W. Zhang, T. Tian, W. Ouyang, P. Wang, S. Wang, Y. Ju and G. Li, *Macromolecules*, 2020, **53**(5), 1842–1851.
16 P. M. Martins, B. Santos, H. Salazar, S. A. C. Carabineiro, G. Botelho, C. J. Tavares and S. Lanceros-Mendez, *Chemosphere*, 2022, **293**, 133548.
17 G. Damonte, R. Spotorno, D. Di Fonzo and O. Monticelli, *ACS Appl. Polym. Mater.*, 2022, **4**(9), 6521–6530.
18 Q. Zhang, D. Qu, B. L. Feringa and H. Tian, *J. Am. Chem. Soc.*, 2022, **144**(5), 2022–2033.
19 A. Khan, R. R. Kisannagar, C. Gouda, D. Gupta and H. C. Lin, *J. Mater. Chem. A*, 2020, **8**(38), 19954–19964.
20 S. J. Tonkin, C. T. Gibson, J. Campbell, D. Lewis, A. Karton, T. Hasell and J. M. Chalker, *Chem. Sci.*, 2020, **11**(21), 5537–5546.
21 Y. J. Wang, S. T. Sun and P. Y. Wu, *Adv. Funct. Mater.*, 2021, **31**(24), 2101494.
22 Z. Chen, N. Gao, Y. Chu, Y. He and Y. Wang, *ACS Appl. Mater. Interfaces*, 2021, **13**(28), 33557–33565.
23 L. Song, B. Zhang, G. Gao, C. S. Xiao and G. Li, *Eur. Polym. J.*, 2019, **115**, 346–355.
24 W. T. Wang, F. Wang, C. Zhang, J. N. Tang, X. R. Zeng and X. J. Wan, *Chem. Eng. J.*, 2021, **404**, 126358.